

A Model for Resonance-Assisted Hydrogen Bonding in Crystals and Its Graph Set Analysis

Robert W. Munn^{*,†} and Craig J. Eckhardt^{*,‡}

Department of Chemistry, UMIST, Manchester M60 1QD, U.K., and Department of Chemistry, University of Nebraska—Lincoln, Lincoln, Nebraska 68588-0304

Received: March 20, 2001

Resonance-assisted hydrogen bonding is treated by the simple quantum-mechanical model of a particle on a ring with different effective masses in the hydrogen bond and in the conjugated segment attached to its ends. The model is applied to an intramolecular hydrogen bond and extended to a hydrogen-bonded dimer and rings of arbitrary size up to an infinite chain of molecules, thus covering the main patterns of bonding identified by graph-set analysis. Analysis of intramolecular hydrogen bonding yields an electron effective mass in the hydrogen bond segment of about 34 electron masses. Conjugation always lowers the energy, but the lowering per molecule decreases with increasing ring size, that for the chain being one-third of that for the intramolecular hydrogen bond. This result rationalizes a predominance of intramolecular hydrogen bonds and dimer rings, given that geometrical factors also affect bonding.

Introduction

The role of hydrogen bonds as a structural organizing feature in chemistry and biology is well-known. In particular, there has been extensive work to classify and interpret the structural motifs associated with hydrogen bonds within and between molecules in crystals. For example, graph-set analysis^{1,2} has been used to identify four basic patterns of hydrogen bonding: an intramolecular or self-bond ring (S), a dimer ring (R), an infinite chain (C), and other finite or discrete patterns (D). Such classification is extremely useful in providing a soundly based taxonomy for describing the diversity of hydrogen bonding patterns in crystals. It would be even more useful if in addition to this codification there were a physical picture of similar scope and generality that would help to interpret and rationalize the observed diversity. The present paper seeks to provide such a model.

The Ferrara group^{3–8} has surveyed experimental results which show that noticeably short hydrogen bonds with the hydrogen atom nearly at the center occur in systems of the general structure $-X-H\cdots X=$, where the two identical X atoms (homonuclear hydrogen bonding) are connected by a conjugated π -electron system. This in turn requires an odd number of atoms in the π system. It is plausible that in such systems the two resonance hybrids of the π system, which require the transfer of the H atom from one X atom to the other, as illustrated in Figure 1, should lead to an equalization of bond lengths not only in the π system, as usual, but also in the hydrogen bond system. More recently, the Ferrara group has also provided evidence that such *resonance-assisted hydrogen bonding* may also occur when the two electronegative atoms X are not the same (heteronuclear hydrogen bonding).^{9–13} Because hydrogen bond strength is exponentially dependent on length,^{14,15} mechanisms for shortening hydrogen bonds are of particular significance.

The substantial theoretical literature on hydrogen bonding has employed both the valence-bond and molecular-orbital models.¹⁶

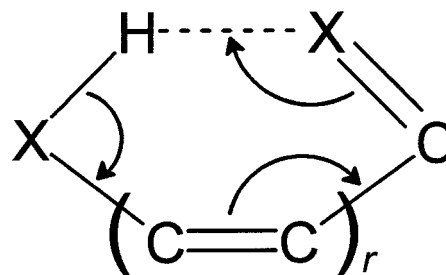


Figure 1. Structural pattern for resonance-assisted hydrogen bonding.

The resonance-assisted mechanism for strong hydrogen bonding starts from the valence-bond model, which has the advantage of permitting the use of curly arrows to show how the resonance hybrids are related. This, of course, is a familiar and productive approach in chemistry. On the other hand, valuable insights into conjugated systems are also obtained from the molecular-orbital model, where delocalization is built in at the start. Some of these insights are available even in highly simplified quantum mechanical models such as the particle in a box or on a ring. The particle in a box model is invoked in elementary chemistry to rationalize such matters as the red shift in optical spectra of conjugated polyenes with increasing chain length. The particle on a ring model is perhaps less familiar but is used in understanding NMR shielding and deshielding at different positions near a benzene ring in terms of a ring current¹⁷ and as the perimeter free electron orbital model in classifying the excited states of aromatic hydrocarbons.¹⁸ Here we explore a highly simplified but useful conceptual model for resonance-assisted hydrogen bonding in terms of a particle on a ring. We consider first the intramolecular hydrogen bond (type S) and then extend the treatment to the dimer (type R) and hence to larger rings, culminating in the infinite ring, which corresponds to the infinite chain (type C) with cyclic boundary conditions. Thus, we treat the three main graph set patterns.

Model for the Intramolecular Hydrogen Bond. For the intramolecular hydrogen bond (type S), the basic model consists of a ring of radius R divided into two segments. One segment that we label b represents the hydrogen bond $-X-H\cdots X=$ and

* To whom correspondence should be addressed.

† UMIST.

‡ University of Nebraska—Lincoln.

the other segment that we label *c* represents the conjugated system that connects the two X atoms. An electron moves in segment *c* with an effective mass m_c and in segment *b* with an effective mass m_b , where the concept of *effective mass* is borrowed from solid-state physics. As explained in standard solid-state physics texts, a particle at the bottom of an energy band moves as though it has a mass determined by the inverse of the curvature of the band, a quantity that may differ markedly from the normal inertial mass of the free particle. Here it allows for the fact that the mobile particle is not an isolated electron but an electron that is interacting with other electrons and with nuclei. In particular, it enables us to use electron transfer in the hydrogen bond as a surrogate or alias for proton transfer from one side to the other of the hydrogen bond, because the two transfers are strongly correlated.¹⁹ We expect $m_b > m_c$, because the transfer of an electron through the hydrogen bond region requires significant movement of the much heavier hydrogen nucleus. In any case, we expect m_b to change markedly if we replace hydrogen by deuterium, thus providing us with a mechanism for an isotope effect.

The position of the electron on the ring is described by an angular variable P ($0 \leq P \leq 2\pi$). The bond segment *b* corresponds to $0 \leq P \leq 2\pi f$ and the conjugated segment *c* to $2\pi f \leq P \leq 2\pi$. Here f is the fraction of the ring that is occupied by the hydrogen bond. This changes with the length of the conjugated system, which is known to modify the hydrogen bond characteristics.^{3–8} The parameters f and R are directly related to the chemical system being considered. The hydrogen-bond segment *c* comprises three atoms and the conjugated segment *c* comprises an odd number of atoms, as Figure 1 indicates. The whole chemical ring therefore comprises an even number of atoms n and, hence, the same number of bonds. Two of these bonds comprise segment *b*, and hence, $f = 2/n$. If we suppose that each bond contributes the same length d to the model ring, then the circumference is nd and $R = nd/2\pi$. One could alternatively treat the chemical ring as a regular polygon with n sides of length d and take the model ring as the circumscribed circle, in which case $R = d/(2 \sin \pi/n)$. For large n , these treatments become equivalent.

The wave function of the system is ψ_b in segment *b* and ψ_c in segment *c*. For energy E , the time-independent Schrödinger equation in the two segments is

$$-\frac{\hbar^2}{2m_b R^2} \frac{\partial^2 \psi_b}{\partial \phi^2} = E \psi_b \quad (1)$$

$$-\frac{\hbar^2}{2m_c R^2} \frac{\partial^2 \psi_c}{\partial \phi^2} = E \psi_c \quad (2)$$

Here $m_b R^2$ corresponds to the moment of inertia of the electron in segment *b* and $m_c R^2$ to that in segment *c*. Set

$$E = L_b^2/2m_b R^2 = L_c^2/2m_c R^2 \quad (3)$$

so that L_b and L_c (which may be positive or negative corresponding to opposite senses of circulation) are the classical angular momenta in segments *b* and *c*, where we shall set $L_b = \rho L_c$ so that $\rho^2 = m_b/m_c$. Then eqs 1 and 2 have solutions

$$\psi_b = \psi_b^0 \exp(iL_b \phi/\hbar) \quad (4)$$

$$\psi_c = \psi_c^0 \exp(iL_c \phi/\hbar) \quad (5)$$

The solutions are subject to the boundary conditions that the

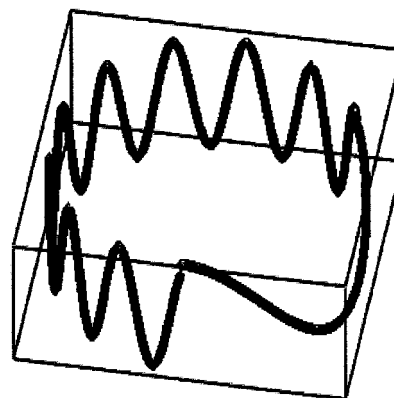


Figure 2. Real part of the wave function for $f = 1/3$ and $\rho = 5$.

wave functions must be equal at the ends where the segments join. The first boundary condition is $\psi_b(0) = \psi_c(2\pi)$, i.e.

$$\psi_b^0 = \psi_c^0 \exp(2\pi i L_c/\hbar) \quad (6)$$

and the second is $\psi_b(2\pi f) = \psi_c(2\pi f)$, i.e.

$$\psi_b^0 \exp(2\pi i f L_b/\hbar) = \psi_c^0 \exp(2\pi i f L_c/\hbar) \quad (7)$$

Substitution from (6) into (7) and expressing L_b in terms of L_c yields

$$\exp[(1 - f + \rho f)(2\pi i L_c/\hbar)] \quad (8)$$

By comparison with the result $\exp(2\pi i k) = 1$ for integer k , we find that the angular momentum in segment *c* must be quantized in the form

$$L_c = \hbar k/(1 - f + \rho f) \quad (9)$$

where k is a nonzero integer. Hence the energy in state k is

$$E_k = \frac{\hbar^2 k^2}{2m_c R^2 (1 - f - \rho f)^2} \quad (10)$$

It follows that a single electron in the lowest level has energy

$$E_1 = \frac{\hbar^2}{2m_c R^2 (1 - f - \rho f)^2} \quad (11)$$

Given the quantized value of the angular momentum L_c , one obtains L_b at once as $\rho > L_c$. From eqs 4–6, the wave function in the two segments is given in terms of L_c by

$$\Psi_c = \Psi_c^0 \exp(iL_c \phi/\hbar) \quad (12)$$

$$\Psi_b = \Psi_c^0 \exp(2\pi i L_c/\hbar) \exp(iL_c \rho \phi/\hbar) \quad (13)$$

The real part of the total wave function for $k = 1$ is plotted in Figure 2 for parameter values $f = 1/3$ (corresponding to one hydrogen bond in a six-membered ring) and $\rho = 5$. In the hydrogen-bonded segment, which lies at the bottom right-hand corner, the wave function ψ_b varies only slowly, but in the conjugated segment, ψ_c varies much more rapidly, owing to the additional factor ρ that multiplies P in eq 13 compared with eq 12.

Usually energy changes are more significant than energies themselves. Here the question is what effect the resonance assistance has on the hydrogen bonding, and therefore, we must

consider the isolated hydrogen bond. In the absence of the conjugated segment of the ring *c*, the hydrogen bond comprises just segment *b*, for which we shall use the label *B* instead of *b*. The wave function in this segment is still given by eq 4, but the boundary conditions become $\psi_B(0) = 0 = \psi_B(2\pi f)$. The solutions in this instance are not traveling waves as those in eqs 4 and 5, but standing waves obtained by combining degenerate solutions (4) with equal and opposite L_B . As for an electron in a box, the solution that satisfies the boundary condition at the origin $\psi_B(0) = 0$ follows if the combination leading to a sine function is taken, i.e.

$$\psi_B = \psi_B^0 \sin(L_B \varphi / \hbar) \quad (14)$$

The other boundary condition $\psi_B(2\pi f) = 0$ yields

$$\sin(2\pi f L_B / \hbar) = 0 \quad (15)$$

and hence L_B must be of the form

$$L_B = \hbar K / f \quad (16)$$

where K is a nonzero integer. The energy is then

$$E_K^0 = \frac{\hbar^2 K^2}{2m_b R^2 f^2} \quad (17)$$

(where the superscript zero denotes the unconjugated hydrogen bond), so that an electron in the lowest level has energy

$$E_1^0 = \frac{\hbar^2}{2m_b R^2 f^2} = \frac{\hbar^2}{2m_c R^2 \rho^2 f^2} \quad (18)$$

We can now compare E_1^0 (without conjugation) with E_1 (with conjugation). Because $f < 1$, E_1 has a larger denominator than E_1^0 and, hence, is smaller. The energy lowering per electron is

$$\Delta E_1 = \frac{\hbar^2}{2m_c R^2} \left[\frac{1}{\rho^2 f^2} - \frac{1}{(\rho f + 1 - f)^2} \right] \quad (19)$$

$$= \frac{\hbar^2}{2m_b R^2} \left[\frac{1}{f^2} - \frac{\rho^2}{(\rho f + 1 - f)^2} \right] \quad (20)$$

This is zero when $f = 1$, because then there is no conjugated segment in either case. It also tends to zero as $\rho f / (1 - f) \rightarrow \infty$ for $f \neq 1$, when the two terms in the square bracket in eq 19 become equal. Increasing ρ , as happens on deuteration, thus reduces the energy lowering produced by the conjugated pathway. Increasing the radius R of the ring can also be seen to reduce the energy lowering.

With f and R expressed in terms of the number of bonds n and the bond length d , the energy lowering per electron becomes

$$\Delta E_1 = \frac{h^2}{8m_b d^2} \left[1 - \frac{4\rho^2}{(n - 2 + 2\rho)^2} \right] \quad (21)$$

For $n \gg \rho$, ΔE_1 reaches its maximum value $h^2/8m_b d^2$, which is just the lowest energy of a particle of mass m_b in a box of length d . Increasing the length of the conjugated chain thus increases the stabilization of the hydrogen bond toward this value.

The Ferrara group characterizes resonance-assisted hydrogen bonds by a parameter λ derived from the bond lengths in the hydrogen-bonded system.³⁻⁸ This parameter ranges from 0 to 1 as the hydrogen bonding varies from complete localization

of the proton on one side to complete localization on the other, so that a value of $1/2$ corresponds to complete delocalization. The present model envisages complete delocalization as one limit, with complete localization on either side as the other. Intermediate situations are represented by a mixture in which the fractional contribution of the delocalized model depends on an auxiliary parameter ξ that we define to equal $4\lambda(1 - \lambda)$, which takes the value unity for $\lambda = 1/2$ and zero for $\lambda = 0$ or 1. The energy lowering relative to completely localized hydrogen bonding is then consistent with Figure 2 in ref 3. This shows that for S-type intramolecular hydrogen bonds the oxygen–oxygen distance (which serves as a surrogate for the hydrogen bond energy) has a dependence on λ that is symmetric about $\lambda = 1/2$ and is roughly parabolic.

We have explored this idea using our model to analyze the data for oxygen–oxygen distances, taking values of the parameter λ from ref 3 and converting the oxygen–oxygen distances to hydrogen bond energies using a procedure described in the literature.⁷ We then examined the hydrogen bond energies as a function of ξ by linear regression against ξ , ξ^2 , and $\sqrt{\xi}$. In practice, owing to the large scatter in the data, all of these simple fits give values of the squared correlation coefficient r^2 of 0.6–0.7, so that none can be preferred on the grounds of a statistically superior fit. However, only the regression on ξ^2 gives a reasonable unconstrained value of the hydrogen bond energy in the absence of resonance assistance (the intercept at $\xi = 0$), namely, 17 kJ mol⁻¹. This is consistent with a model in which ξ determines the contribution from the conjugated structure to the wave function, because then ξ^2 determines the contribution to the energy. For this plot, the slope is 52 kJ mol⁻¹, which we equate to $2\Delta E_1$ for two electrons in the bond. We have ΔE_1 given by eq 21, in which $n = 6$ ($f = 1/3$) for the structures under investigation, for which we take $d = 1.344$ Å as the average bond length in the unperturbed geometry.³

Taking m_c as the usual electron inertial mass m_e leads finally to a value of $\rho = 5.85$, so that the effective mass of the electron in the hydrogen bond segment is $m_b = 34.2m_e$. Clearly, this is much higher than the electron inertial mass but much lower than the inertial mass of the proton, $m_p = 1836m_e$. This is consistent with the use of the electron motion as a surrogate for the proton motion, where the effective mass represents the curvature of the potential energy in which the electron moves and hence differs from the inertial mass. In our model, the electron that represents the proton certainly moves more slowly than a normal electron, but the reduction is less than the ratio of the proton and electron inertial masses would suggest, implying that the electron movement takes place in a rather flat effective potential.

We can also compare our results for the ring with the two segments with those for a simple conjugated ring of the same size in which two more conjugated bonds replace the hydrogen-bonded segment. In such systems, the ring current model¹⁷ affords insights into the NMR spectrum. Applying a magnetic field perpendicular to the ring induces a circulation of current around the ring equivalent to an induced magnetic dipole moment. This induced moment produces an additional magnetic field that deshields nuclei outside the ring (and shields nuclei inside it, such as the protons held over the ring in *paracyclophanes*) to an extent that depends inversely on the effective mass of the circulating electrons. For the simple conjugated ring, with no hydrogen bond, the energy in the lowest level is obtained from eq 10 with $f = 0$. Comparison with eq 10 itself, describing the ring with the hydrogen bond, shows that the effective mass has been increased by the factor $(1 - f + \rho f)^2$.

It follows as a prediction from our model that the deshielding of nuclei outside the ring with the hydrogen bond should be reduced by this factor relative to a simple conjugated ring of the same size. As noted earlier, deuteration increases ρ , which reduces deshielding still further. On the other hand, stronger hydrogen bonds have lower energies that correspond to reduced values of ρ and, hence, lead to less reduction in the deshielding. The Ferrara group has reported a strong correlation between proton NMR shifts and hydrogen bond strength,⁸ but this concerns the hydrogen atom that forms part of the hydrogen-bonded system. In our model, this atom is considered as lying on the ring rather than outside it, and the ring-current model is then uninformative.

Extension to Hydrogen-Bonded Dimers and Beyond. We now consider the extension of our treatment to a hydrogen-bonded dimer (type R) comprising two conjugated segments, labeled c1 and c2, and two hydrogen-bonded segments, labeled b1 and b2. To make comparisons with the intramolecular hydrogen bond for the monomer, we take a total of n atoms for each molecule, of which three form each hydrogen bond. Hence, there are $2n$ atoms and $2n$ bonds in total, with two hydrogen-bonded segments of two bonds each. As a result, each segment b1 and b2 occupies a fraction $1/n$ of the whole ring, whereas together they occupy the fraction $f = 2/n$, the same as that for the intramolecular hydrogen bond. Corresponding segments are equivalent, so the effective masses are the same as before: m_c in the conjugated segments and m_b in the hydrogen bond segments.

In the different segments, the wave functions are ψ_{bi} and ψ_{ci} , where $i = 1$ or 2 . They obey Schrödinger equations such as (1) and (2) which we solve as before by expressing the energy E in terms of classical angular momenta to obtain solutions of the forms (4) and (5) and applying suitable boundary conditions. The boundary conditions at the hydrogen bonds between different molecules are $\psi_{b1}(0) = \psi_{c2}(2\pi)$ and $\psi_{c1}(\pi) = \psi_{b2}(\pi)$, whereas those within the individual molecules are $\psi_{b1}(\pi f) = \psi_{c1}(\pi f)$ and $\psi_{b2}(\pi + \pi f) = \psi_{c2}(\pi + \pi f)$. Note that, for ease of comparison, the fraction f is defined to be the same as that for the monomer: each hydrogen bond subtends half the angle it did in the monomer, but this is the same fraction f of π , which is half the total angle 2π . The procedures applied for the monomer then lead to exactly the same quantization condition as before, eq 9. The primary difference from the monomer case is that the size of the ring is doubled for the dimer, and as a result, the energy eigenvalues are all a factor of 4 smaller than those in the monomer.

From this derivation, it follows that extension to a ring of N monomers would simply result in reducing all of the energy eigenvalues by a factor of N^2 . In the limit $N \rightarrow \infty$, we obtain the result for an infinite chain (with the common device of cyclic boundary conditions), which is type C.

To compare the results for the dimer and larger rings with those for the monomer, we have to consider how to populate the energy levels. For the monomer, a valence-bond description of switching the hydrogen bond from one side to the other of segment b requires the movement of a pair of electrons. These can be accommodated in the degenerate states of lowest energy, which have quantum numbers ± 1 corresponding to opposite senses of movement. Together these yield a standing wave rather than a traveling wave with one nodal line across the ring. Movement of just one pair of electrons can also switch all of the hydrogen bonds simultaneously for any number of molecules conjugated in a ring. On the other hand, it seems that the relevant comparison must consider the energy lowering per molecule

produced by the conjugated pathway in rings of different size, and this requires movement of one pair of electrons per molecule. This can be regarded as representing a process of switching one hydrogen bond per molecule. Then for N molecules there are two electrons in each of the lowest energy levels up to and including those with quantum numbers $\pm N$. This yields standing waves with 1 to N nodal lines across the ring.

The total energy lowering for a ring of N molecules populated by $2N$ electrons is then found by adapting eq 21 to be

$$\frac{\Delta E}{N} = \frac{2}{N} \frac{h^2}{8m_b(Nd)^2} \left[1 - \frac{4\rho^2}{(n-2+2\rho)^2} \right] (1^2 + 2^2 + \dots + N^2) \quad (22)$$

$$= \frac{h^2}{4m_b d^2} \left[1 - \frac{4\rho^2}{(n-2+2\rho)^2} \right] \frac{(N+1)(2N+1)}{6N^2} \quad (23)$$

The function of N on the right-hand side of eq 23 is equal to 1 for $N = 1$ and tends to $1/3$ as $N \rightarrow \infty$. Hence, there is a significant energy lowering caused by conjugation for rings of all sizes, but the intramolecular hydrogen-bonded monomer and smaller rings are favored, all things being equal. This conclusion is broadly consistent with the hydrogen bond lengths tabulated by the Ferrara group, which tend to be larger in chains⁷ than in intramolecular rings,⁸ hence, implying greater stability of the latter.

Discussion

We have treated a very simple model of a particle on a ring that comprises two different kinds of segments corresponding to conjugated paths and hydrogen bonds with different effective masses in the different kinds of segments. Although the model is simple, solving it and deducing its consequences for different graph set patterns requires detailed analysis. We have shown that the conjugation lowers the energy, consistent with the Ferrara group's concept of resonance-assisted hydrogen bonding,³⁻⁸ and that the model can fit data for intramolecular bonds of type S with an electron effective mass in the hydrogen bond segment of some 34 electron inertial masses. Using effective mass in the context of hydrogen bonding is unusual but is helpful conceptually. For example, it serves to give the proton an implicit role in resonance-assisted hydrogen bonding by its effect on the electron dynamics. The effective mass also indicates the relative flatness of the hydrogen bond potential, and presumably takes some account of proton tunneling. The present model for a hydrogen-bonded ring of molecules is conceptually similar to the coordinated proton tunneling observed by NMR relaxometry in a calixarene,²⁰ although in that case no conjugated segments intervened between the four hydrogen bonds.

The energy lowering applies not only to a simple intramolecular hydrogen bond but also to a hydrogen-bonded dimer and larger rings that in the limit become an infinite chain. In practice, geometrical constraints on bonding will govern which structure may reasonably occur, but our results indicate that an intramolecular ring or a dimer will tend to be favored, consistent with the graph-set classification that identifies such types of hydrogen bonding (S and R) separately from chains (C) and others (D). In our analysis, the chain is least favored, but this structural feature may benefit from other favorable factors such as the cooperative effect in α helices, whereby it becomes easier to form second and subsequent hydrogen bonds.²¹ For example, a molecular orbital comparison between hydrogen-bonded chains of urea molecules and chains of 1,3-propanedione molecules²²

indicates that the resonance-assisted mechanism is more important where covalent rather than electrostatic interactions prevail.

Our treatment is most likely to be relevant to homonuclear hydrogen bonds with the same electronegative atom at either end, as originally discussed by the Ferrara group.^{3–8} However, the qualitative effects are likely to be the same for heteronuclear hydrogen bonds with different atoms at either end.^{9–13} This would imply less delocalization, i.e., a value of the parameter λ introduced earlier that departs from $1/2$, and presumably a modified value of the effective mass m_b . It would also imply a correspondingly more ionic rather than covalent structure²² that would rather stretch the validity of the model. Nevertheless, such an extension should be valuable in providing extended interpretation.

Acknowledgment. This work was stimulated by the NATO Advanced Research Workshop “Crystals: Supra-molecular Materials”. We are grateful to the Organizing Committee for invitations and support to attend this meeting.

References and Notes

- (1) Etter, M. C.; MacDonald, J. C.; Bernstein, J. *Acta Crystallogr. B* **1990**, *46*, 256–262.
- (2) Bernstein, J.; Davis, R. E.; Shimoni, L.; Chang, N.-L. *Angew. Chem., Int. Ed. Engl.* **1995**, *34*, 1555–1573.
- (3) Gilli, G.; Bellucci, F.; Ferretti, V.; Bertolasi, V. *J. Am. Chem. Soc.* **1989**, *111*, 1023–1028.
- (4) Bertolasi, V.; Gilli, P.; Ferretti, V.; Gilli, G. *J. Am. Chem. Soc.* **1991**, *113*, 4917–4925.
- (5) Gilli, G.; Bertolasi, V.; Ferretti, V.; Gilli, P. *Acta Crystallogr. B* **1993**, *49*, 564–576.
- (6) Gilli, P.; Bertolasi, V.; Ferretti, V.; Gilli, G. *J. Am. Chem. Soc.* **1994**, *116*, 909–915.
- (7) Bertolasi, V.; Gilli, P.; Ferretti, V.; Gilli, G. *Chem.—Eur. J.* **1996**, *2*, 925–934.
- (8) Bertolasi, V.; Gilli, P.; Ferretti, V.; Gilli, G. *J. Chem. Soc., Perkin Trans. 2* **1997**, 945–952.
- (9) Bertolasi, V.; Ferretti, V.; Gilli, P.; Gilli, G.; Issa, Y. M.; Sherif, O. E. *J. Chem. Soc., Perkin Trans. 2* **1993**, 2223–2228.
- (10) Bertolasi, V.; Nanni, L.; Gilli, P.; Ferretti, V.; Gilli, G.; Issa, Y. M.; Sherif, O. E. *New J. Chem.* **1994**, *18*, 251–261.
- (11) Bertolasi, V.; Gilli, P.; Ferretti, V.; Gilli, G. *Acta Crystallogr. B* **1994**, *50*, 617–625.
- (12) Bertolasi, V.; Gilli, P.; Ferretti, V.; Gilli, G. *Acta Crystallogr. B* **1995**, *51*, 1004–1015.
- (13) Bertolasi, V.; Gilli, P.; Ferretti, V.; Gilli, G. *Acta Crystallogr. B* **1998**, *54*, 50–655.
- (14) Espinosa, E.; Molins, E.; Lecomte, C. *Chem. Phys. Lett.* **1998**, 285, 170–173.
- (15) Spackman, M. A. *Chem. Phys. Lett.* **1999**, *301*, 425–429.
- (16) Smith, D. A., Ed.; *Modeling the Hydrogen Bond. ACS Symposium Series, Vol. 569*; American Chemical Society: Washington, DC, 1994. Scheiner, S. *Hydrogen Bonding*; Oxford University Press: New York, 1997.
- (17) Pople, J. A. *J. Chem. Phys.* **1956**, *24*, 1111.
- (18) Platt, J. R. *J. Chem. Phys.* **1949**, *17*, 484–495.
- (19) This situation resembles the old token system used on single-track sections of a railroad to ensure that only one train can enter the section at a time. At the beginning of the section, the locomotive engineer receives a token that permits the train to travel to the other end, where the token is left for the next train in the opposite direction. Although the significant movement is that of the train, it can be monitored (aliased) by the corresponding movement of the token.
- (20) Brougham, D. F.; Caciuffo, R.; Horsewill, A. J. *Nature* **1999**, 397, 241–243.
- (21) Milner-White, E. J. *Protein Sci.* **1997**, *6*, 2477–2481.
- (22) Dannenberg, J. J.; Haskamp, L.; Masunov, Artëm. *J. Phys. Chem. A* **1999**, *103*, 7083–7086.